第 30 卷第 3 期
2013 年 3 月
控 制 理 论 与 应 用
Control Theory & Applications
Vol. 30 No. 3
Mar. 2013

DOI: 10.7641/CTA.2013.12053

采用惯性测量单元的移动机器人轨迹跟踪方法研究

张 弛†

(南京理工大学 机械工程学院, 江苏 南京 210094)

摘要: 对于非完整移动机器人的轨迹跟踪控制已有很多方法提出, 但是这些方法或者是基于动力学模型或者是采用复杂的运动学模型, 对于缺少强大计算设备且需要实时控制的工程应用是不适合的. 本文针对非完整移动机器人提出了一种基于比例微分(proportional-differential, PD)控制器的实时轨迹跟踪控制方法. 该方法运行在40 MHz的嵌入式控制器上的控制周期只有1∼2 ms. 通过将一个用于直流电机控制的非线性PID 速度控制器与提出的轨迹控制器进行集成, 实现了一个轮式移动机器人的运动控制. 机器人轨迹跟踪实验系统中采用微机电系统(micro electro-mechanical system, MEMS)惯性测量单元检测轮式移动机器人的偏航角, 实验结果验证了提出方法的有效性.

关键词: 轨迹跟踪; PD控制器; 轮式移动机器人

中图分类号: TP273 **文献标识码**: A

Path tracking of a mobile robot using inertial measurement unit

ZHANG Chi†

(Mechanical Engineering College, Nanjing University of Science and Technology, Nanjing Jiangsu 210094, China)

Abstract: Many approaches for trajectory tracking of nonholonomic mobile robots have been proposed. Most of them are designed based on the control of robot dynamics or adopt the complicated kinematics control, which are not suitable for real-time engineering applications without powerful computing devices. A real-time tracking controller based on PD controller is presented for nonholonomic mobile robot. This algorithm holds a time cost of only 1∼2 ms for each control loop in a 40 MHz embedded controller. A nonlinear-PID based velocity controller for DC driving motors is integrated with the proposed tracking controller to fulfill the path tracking control of a wheeled mobile robot (WMR). To estimate the yaw angle of WMR, a low-cost micro electro-mechanical system (MEMS) measurement unit is employed in the experimental setup. The experimental results show the effectiveness of the proposed method.

Key words: trajectory tracking; PD controller; wheeled mobile robot

1 Introduction

Because of the complexity brought by nonholonomic constraints, the control of mobile robots has attracted considerable attention in recent years. Several controllers were proposed for mobile robots with nonholonomic constraints, and posture stabilization and trajectory tracking were mainly discussed. The purpose of posture stabilization is to stabilize the robot to a reference point, while the aim of trajectory tracking is to let the robot follow a reference trajectory. With the stabilization problem, trajectory tracking is a more practical issue for mobile robots. Many researchers have studied the controllers for trajectory tracking of nonholonomic mobile robots, which can be divided into two types: one utilizes the kinematic trajectory tracking controller[1–10] to handle only tracking issue, while the other integrates the kinematic trajectory tracking controller with the dynamic controller of the wheeled mobile robot (WMR)[11].

For the kinematic control, there are trajectory tracking methods such as linearization kinematic models[1], input-output linearization[2], feedback control[3], dynamic linearization[4–5], recursive technique[6], sliding-mode[7], and backstepping approach[8–9], fuzzy control[12]. An interesting experimental comparison between control laws proposed in literature has been presented in[11]. Other researchers dealt with the backstepping control architecture[13], the hybrid of the kinematic control and the dynamic controller, and put forward trajectory tracking methods. The backstepping control architecture is frequently applied to practical applications recently[13–23]. To deal with the un-modeled disturbance and parameter uncertainty of the dynamics, neural networks[14–16], adaptive control[17–19], and sliding-mode control (SMC)[20–23] are widely adopted. In literature, a few experimental setups and results can be found; most of them[11, 16, 23–24] consist of a vision system for pose measurement, a host PC for the calculation of the con-

Received 13 March 2012; revised 18 January 2013.

†Corresponding author. Tel.: +86 13910207748.

trol law, and a WMR with a low level controller for executing the control actions.

Although the kinematic controllers are easy to be implemented, most of them are only validated by simulations. The “perfect velocity tracking” assumption[1] of the kinematics controllers may not hold in practice. Other controllers that have considered the dynamics can achieve better motion performance, and the effects of disturbance and parameter uncertainty can be eliminated. However, the complexity of such controllers requires a high computation cost.

This paper focuses its attention to solve the problem of path tracking, guaranteeing the effectiveness and the real-time characteristic simultaneously. An important difference between path following and path tracking lies in the time dependence: path following is to pursue waypoints lying on the desired path, while path tracking is to track a time-parameterized reference path. Among the recent papers addressing path tracking control, [25] extended the preliminary work[26] by concerning the next bend ahead of the vehicle and combining a velocity controller, while [27] presented a higher level waypoints by tracking controller taking position, heading, and current velocity of the robot into the calculation module. The technique proposed in [28] tracks piece-wise linear paths which are an approximation of the feasible smooth reference path. Both [26] and [27] presented their experimental results.

Being different from those above controllers, the proposed tracking controller in this paper considers a human-like tracker-guide mode and implements it in a PD controller. Thus, it is more suitable for engineering applications. Besides, unlike those existing experimental setups, we adopt a self-designed WMR with low performance motors, and the control algorithm is implemented in a 40 MHz ARM chip-based control board instead of a powerful PC.

The organization of the remaining part of the paper is as follows. Section II is a concise description of the kinematical modeling of a differentially steered WMR. In Section III, the design of the proposed tracking controller and the low-level velocity controller are introduced. Section IV gives the detail of yaw angle estimation of WMR using a low-cost inertial measurement unit (IMU). In Section V, real time experimental results of the proposed controller are presented for several trajectories. Section VI draws the conclusions.

2 Modeling

Consider a typical model of the differential-drive WMR consisting of a vehicle with two driving wheels mounted on the same axis and a free front wheel, while two DC motors provide necessary torques for the motion and orientation. With a symmetry structure, the barycenter of the WMR is assumed to be located in the middle of two driving wheels. The following is the kinematic model for the wheeled mobile robot with nonholonomic constraints of pure rolling without slipping phenomenon.

$$\begin{pmatrix} \dot{x} \\ \dot{y} \\ \dot{\theta} \end{pmatrix} = \begin{pmatrix} \cos\theta & 0 \\ \sin\theta & 0 \\ 0 & 1 \end{pmatrix} \cdot \begin{pmatrix} v \\ \omega \end{pmatrix} = \boldsymbol{J}(\theta) \cdot \boldsymbol{V}, \quad (1)$$

where $\boldsymbol{J(\theta)} \in \mathbb{R}^{3\times 2}$ and $\boldsymbol{V} \in \mathbb{R}^2$ are the full rank velocity transformation matrix and velocity vector, respectively. v is the linear velocity and ω is the angular velocity. (x, y) and $(\dot{x}, \dot{y})$ are the actual position and translational velocity of the centroid of WMR in the inertial coordinate system, respectively. θ is the angle between X axis and X_c axis and represents the heading direction, and $\dot{\theta}$ is the angular velocity.

The angular velocities of the right actuated wheel and the left actuated wheel are denoted by $\omega_{\rm r}$ and $\omega_{\rm l}$, respectively. Velocity conversion matrix between $(\omega_{\rm r}, \omega_{\rm l})$ and (v, ω) is given by

$$\begin{pmatrix} \omega_{\rm r} \\ \omega_{\rm l} \end{pmatrix} = \begin{pmatrix} 1/r & d/r \\ 1/r & -d/r \end{pmatrix} \cdot \begin{pmatrix} v \\ \omega \end{pmatrix}, \quad (2)$$

where d is the half of the width of mobile robot, and r denotes the radius of the wheel.

3 Path tracking controller

In Fig.1, we present a path tracking strategy based on PD control method. This kinematics controller consists of a tracking controller and a low-level velocity controller. The tracking controller is designed based on PD control strategy while the low-level velocity controller is implemented based on a nonlinear PID controller.

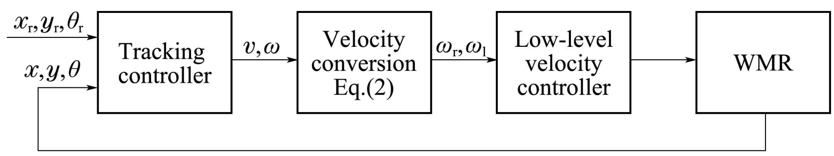

Fig. 1 Kinematics controller for the path tracking of WMR

As shown in Fig.2, a reference robot denoted by the configurations $(x_{\mathrm{r}}, y_{\mathrm{r}}, \theta_{\mathrm{r}})$ moves along the desired path with a specified velocity v_{r}; the real robot denoted by the configurations (x, y, θ) aims to catch up with the reference one. There is an important concept called 'sight-line-angle' (e_{o} in Fig.2) which is used in this path tracking strategy for replacing the heading angle error $\theta_{\mathrm{r}} - \theta$ in most known strategies. To reduce the distance error e_{p} and the 'sight-line-angle' e_{o}, the PD control law is designed as follows:

$$\begin{cases} v = k_{\mathrm{pp}} e_{\mathrm{p}} + k_{\mathrm{dp}} \dot{e}_{\mathrm{p}}, \\ \omega = k_{\mathrm{po}} e_{\mathrm{o}} + k_{\mathrm{do}} \dot{e}_{\mathrm{o}} \end{cases} \tag{3}$$

with

$$\begin{cases} e_{\mathrm{p}} = \sqrt{(x_{\mathrm{r}} - x)^2 + (y_{\mathrm{r}} - y)^2}, \\ e_{\mathrm{o}} = \theta - \text{angle}[(x_{\mathrm{r}} - x) + \mathrm{i}(y_{\mathrm{r}} - y)], \end{cases} \tag{4}$$

where the function angle$[\cdot]$ denotes the argument of the complex number, v and ω represent the velocity input and angular velocity input respectively; $k_{\mathrm{pp}}, k_{\mathrm{dp}}, k_{\mathrm{po}}$ and $k_{\mathrm{do}} > 0$ are the control gains which need to be determined by using the trial and error method.

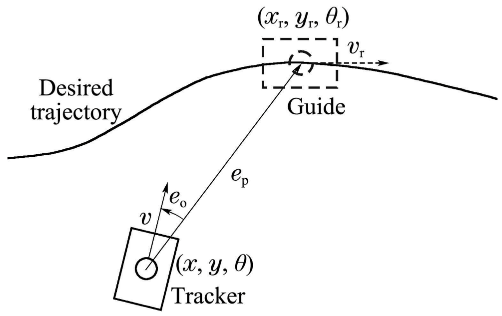

Fig. 2 Diagram of path tracking scheme

In equation (3), we decouple the control problem into two parts: one is to reduce the distance between the real robot and the reference robot, the other is to reduce the 'sight-line-angle'. That strategy is similar to the human tracking mode according to our life experience. Once the distance and the 'sight-line-angle' are eliminated simultaneously, the tracker robot can catch up with the guide one.

From Fig.1, it can be seen that the tracking controller requires angular velocities of two actuated wheels as control inputs of the low-level velocity controller. A nonlinear PID control strategy is implemented to design the velocity controller. Several known amelioration technologies, including incomplete differential, variable-integrator and nonlinear proportion are applied. Combing with those technologies, we design the nonlinear PID controller as follows:

$$\begin{cases} K_{\mathrm{P}} = k_{\mathrm{p}} + b_{\mathrm{p}}[1 - \dfrac{1}{\cosh(a_{\mathrm{p}} \cdot \mathrm{err}(k))}], \\ K_{\mathrm{I}} = k_{\mathrm{i}}[1 - \tanh \dfrac{a_{\mathrm{i}}|\mathrm{err}(k)|}{y_{\max}}], \\ u_{\mathrm{D}}(k) = \alpha u_{\mathrm{D}}(k-1) + k_{\mathrm{d}}(1-\alpha)(\mathrm{err}(k) - \\ \qquad \mathrm{err}(k-1)), \\ u(k) = K_{\mathrm{p}} \cdot \mathrm{err}(k) + K_{\mathrm{I}} \cdot \sum \mathrm{err}(k) + u_{\mathrm{D}}(k), \end{cases} \tag{5}$$

where $k_{\mathrm{p}}, k_{\mathrm{i}}$ and k_{d} denote the parameters of a traditional PID controller, b_{p}, a_{p}, $a_{\mathrm{i}} > 0$ are parameters to be adjusted via the trial and error method, $y_{\max}$ is the maximum output of the system, $0 < \alpha < 1$ should be tuned in applications, $\mathrm{err}(k)$ is the feedback error at the kth sample time, $u(k)$ represents the current control output.

For the tuning of control parameters in the nonlinear PID controller, we adopt the trial and error method. First, we choose values of k_{p} and k_{i} based on our experience; If the control effect is not satisfied, try to change those two values until the dynamic response of system meet the performance requirement. In case of the derivation action, the tuned k_{p} and k_{i} should be decreased a bit and then repeat the trial and error until the optimum values of k_{p}, k_{i} and k_{d} are found. Moreover, the other carefully adjusted control parameters, a_{p}, b_{p}, a_{i}, α can guarantee better control effects but would not have a great impact on the control effectiveness. Then in tuning, those parameters can be chosen in a wide range.

In the velocity controller, the velocity estimation is a critical issue when using a low-quality position measurement device, i.e., in our developed WMR, the photoelectric encoder of the driving motor has only 16 lines. The differential signal obtained by the backward difference (BD) method is very noisy which limits the overall performance[29–30]. In view of that case, a tracking differentiator (TD) method[31] is implemented to provide a high-quality differential signal for more effective and robust performance in the presence of measurement noise. The viability for practical applications has been demonstrated via simulations and experiments[29–30, 32–33].

For a boundary integrable function $r(t)$, system (6) can be used as a high-performance TD to provide two signals $r_1(t)$ and $r_2(t)$: $r_1(t) \to r(t)$ and $r_2(t) \to \dot{r}(t)$, respectively[31]:

$$\begin{cases} r_1(k+1) = r_1(k) + h \cdot r_2(k), \\ r_2(k+1) = \\ r_2(k) + h \cdot fst(r_1(k) - r(k), r_2(k), \delta, h), \end{cases} \tag{6}$$

where h is the sampling step, and δ is a velocity factor that determines the transition. The function $fst(x_1, x_2, \delta, h)$ is defined in the following:

$$fst(x_1, x_2, \delta, h) = -\begin{cases} \delta \mathrm{sgn}\, a, & |a| > d, \\ \delta \dfrac{a}{d}, & |a| \leqslant d \end{cases} \tag{7}$$

where, sgn denotes the SIGN function, a and d can be determined as follows:

$$a = \begin{cases} x_2 + \dfrac{a_0 - d}{2} \mathrm{sgn}\, y, & |y| > d_0, \\ x_2 + \dfrac{y}{h}, & |y| \leqslant d_0 \end{cases} \tag{8}$$

with

$$\begin{cases} d = \delta \cdot h, \\ d_0 = h \cdot d, \\ y = x_1 + h \cdot x_2, \\ a_0 = \sqrt{d^2 + 8\delta |y|}. \end{cases} \tag{9}$$

4 Yaw angle estimation

An important issue in the feedback control of the robot is the estimation of yaw angle θ. we adopted a simple complementary filter to estimate the attitude[12]. We can take advantage of the gyroscope sensor's accuracy over short time and the accelerometer's stability over long time to produce angle calculations that are stable over both short and long time periods. The approach can be described as follows:

1) Use the gyro sensor to measure angle changes on short time scales, which is expressed as

$$\theta_{\mathrm{gyro}}(n) = \theta_{\mathrm{e}}(n-1) + w \cdot \mathrm{d}t, \tag{10}$$

where $\theta_{\mathrm{gyro}}(n)$ is the angle calculated from gyro sensor at the present moment, $\theta_{\mathrm{e}}(n-1)$ is the estimated angle at the last moment. Moreover, w, $\mathrm{d}t$ are the angle velocity measured from gyro sensor and the compute period, respectively.

2) Use the accelerometer as a tilt sensor to calculate the tilt angles.

3) Fuse the angles derived from the gyro sensor with the magnetic angles over a long time scale.

$$\begin{aligned} \theta_{\mathrm{e}}(n) &= \theta_{\mathrm{gyro}}(n) + e(n), \\ e(n) &= K(\theta_{\mathrm{acc}}(n) - \theta_{\mathrm{gyro}}(n)), \end{aligned} \tag{11}$$

where, $\theta_{\mathrm{acc}}(n)$ is the angle calculated from magnetic meter at the present moment, K is a positive constant, which decides the proportion of the values of gyro and magnetic meter.

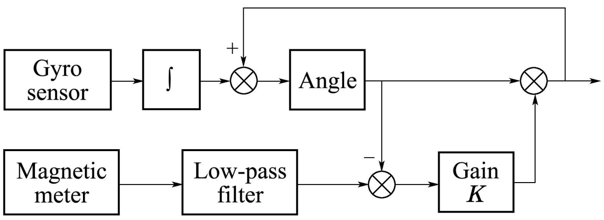

Fig. 3 Structure of estimate algorithm

A low pass filter is added to avoid vibration from motor on the influence of the magnetic meter. The complementary filter strategy is shown as Fig.3.

5 Experimental studies

The experimental setup is shown in Fig.4. It consists of a real-time vision system[34], a wireless communication system, a navigation module and a motion controller. In the vision system, these following equipment are included: a CP–480 camera manufactured by PANASONIC® is used to capture the image; an image processing card QP300 manufactured by DAHENG® is adapted to grab real-time image data and to transmit them to an external interface or displayed RAM. For the communication system, a Xbee-Pro II wireless RF module provided by Digi International® is integrated for the communication between the WMR and the host computer. The navigation module employs a low-cost inertial sensor to estimate the yaw angle, θ. The motion controller installed on the WMR is designed based on a 40 MHz Cortex–M3 chip, LM3S2965, manufactured by TI®.

Fig. 4 Overview of the experimental setup

Table 1 System parameters of the WMR

Parameter	Description	Nominal value
m	Mass of the WMR	3.3 kg
r	Radius of the wheels	0.08 m
d	Distance between the two driven wheels	0.28 m
l	Longitudinal length of the WMR	0.3 m
$v_{\max}$	Maximum forward velocity of the WMR	0.4 m/s
$\omega_{\max}$	Maximum steering velocity of the WMR	1.33 rad/s
T_1	Control period of the velocity controller	20 ms
T_2	Control period of the tracking controller	100 ms

System parameters of the WMR are shown in Table 1 and control gains of the controllers are given in Table 2. Two basic types of paths are tracked in experiments: straight line and circle. Owing to the limitation of the area of vision field, 2.1 m×2.1 m, the desired forward velocity is specified to be 0.1 m/s. The initial posture of the WMR is $\boldsymbol{q}(0) = [x(0)\ \ y(0)\ \ \theta(0)]^{\mathrm{T}} = [0\ \ 0\ \ 0]^{\mathrm{T}}$.

Table 2 Control gains of the controllers

Nonlinear PID controller	$k_{\mathrm{p}}, k_{\mathrm{i}}, k_{\mathrm{d}}$	1.2, 0.25, 1.0
	$a_{\mathrm{p}}, b_{\mathrm{p}}$	0.8, 1.0
	a_{i}	1.6
	α	0.8
Tracking differentiator	h	0.02
	δ	5500

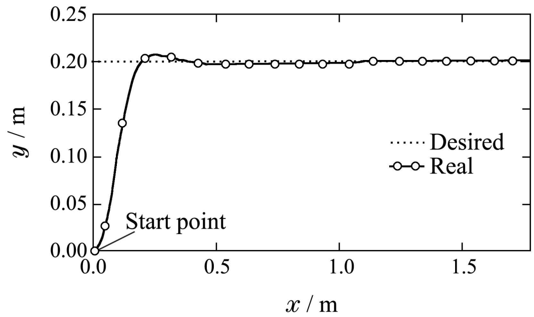

Fig. 5 Experimental result for the straight line tracking

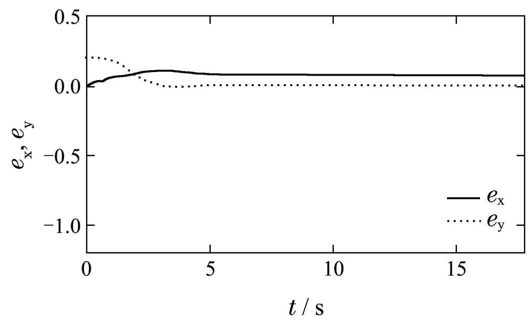

Fig. 6 Position errors for the straight line tracking

1) Results for the straight line path. In this experiment, the WMR follows the trajectory as denoted by the dashed line in Fig.5. Although a big initial position error exists, the robot quickly reduces this error under the control with a very small overshoot less than 0.01 m. As the robot catches up with the desired straight line trajectory, the orientation of the robot also approximates the desired value $\theta_{\mathrm{r}} = 0$. As it can be seen in Fig.6, the position error along X axis, $e_{\mathrm{x}} = x_{\mathrm{r}} - x$, converges to a steady value less than 0.08 m, while the position error along Y axis, $e_{\mathrm{y}} = y_{\mathrm{r}} - y$, converges to 0. In practical applications, a tracking error less than 0.08 m is acceptable in real exploration applications.

2) Results for the circle path: The desired circle trajectory can be seen from Fig.7, the radius of which is 0.5 m. With the proposed controller (3), the robot can quickly catch up the desired motion in 4 s without overshoot even though an initial position error exists. As can be seen in Fig.8, the steady position error is less than 0.04 m.

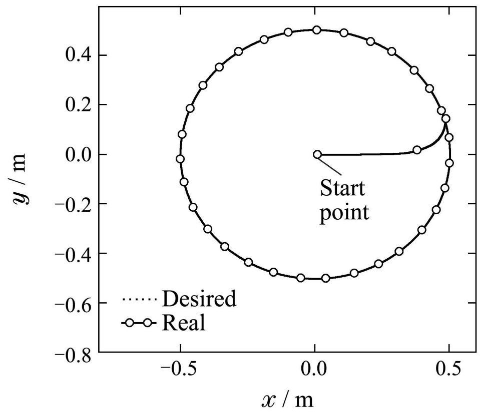

Fig. 7 Experimental result for the circle tracking

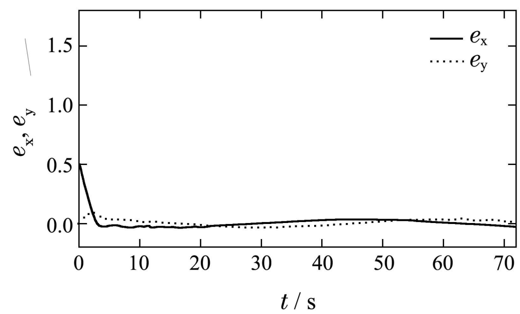

Fig. 8 Position errors for the circle tracking

6 Conclusions

A path tracking strategy for the nonholonomic mobile robot based on a PD controller is proposed. It mimics the humanlike 'tracker and guide' mode. Unlike known tracking methods, the proposed strategy takes the distance and the 'sight-line-angle' as the control inputs. Besides, to achieve the low-level velocity control, we also implement a nonlinear PID controller. For the estimation of the yaw angle of robot, a low-cost IMU is employed in the experimental setup. Two basic Path tracking experiments verify the effectiveness of the proposed tracking strategy and the low-level velocity controller. Of course, more engineering application experiments are required to confirm the practical value of the proposed approach.

References:

[1] KANNAYAMA Y, KIMURA Y, MIYAZAKI F, et al. A stable tracking control method for an autonomous mobile robot [C] //*Proceedings of IEEE International Conference Robotics Automation*. Cincinnati: IEEE, 1990: 384 – 389.

[2] KIM D H, OH T H. Tracking control of a two-wheeled mobile robot using input-output linearization [J]. *Control Engineering Practice*, 1999, 7(3): 369 – 373.

[3] SAMSON C, ABDERRAHIM K A. Feedback control of a nonholonomic wheeled cart in Cartesian space [C] //*Procedings of IEEE International Conference of Robotics and Automation*. Sacramento: IEEE, 1991: 1136 – 1141.

[4] NOVEL ANDREA B D, BASTIN G, CAMPION G. Control of nonholonomic wheeled mobile robots by state feedback linearization [J]. *International Journal of Robotics Research*, 1995, 14(6): 543 – 559.

[5] ORIOLO G, DE LUCA A, VENDITTELLI M. WMR control via dynamic feedback linearization: Design, implementation, and experimental validation [J]. *IEEE Transaction on Control Systems Technology*, 2002, 10(3): 835 – 852.

[6] JIANG Z P, NIJMEIJER H. A recursive technique for tracking control of nonholonomic system in chained form [J]. *IEEE Transaction on Automatic Control*, 1999, 44(2): 265 – 279.

[7] BLOCH A, DRAKUNOV S. Tracking in nonholonomic dynamic system via sliding-modes [C] //*Proceedings of IEEE Conference of Decision Control*. New Orleans, IEEE, 1995: 2103 – 2106.

[8] LEE T C, SONG K T, LEE C H, et al. Tracking control of unicycle-modeled mobile robots using a saturation feedback controller [J]. *IEEE Transactions on Control Systems Technology*, 2001, 9(2): 305 – 318.

[9] JIANG Z P, NIJMEIJEV H. Tracking control mobile robots: a case study in backstepping [J]. *Automatica*, 1997, 33(7): 1393 – 1399.

[10] ZHAO Y, BEMENT S L. Kinematics, dynamics and control of wheeled mobile robots [C] //*Proceedings of IEEE International Conference of Robotics and Automation*. Nice: IEEE, 1992: 91 – 96.

[11] KIM B, TSIOTRAS P. Controllers for unicycle-type wheeled robots: theoretical results and experimental validation [J]. *IEEE Transaction on Robotics and Automation*, 2002,18(3): 294 – 307.

[12] GAO Xingquan, CHEN Hong. Tracking control for wheeled mobile robot via T–S fuzzy model [J]. *Control Theory & Applications*, 2007, 24(6): 873 – 878.
(高兴泉, 陈虹. 基于T–S模型的轮式移动机器人轨迹跟踪控制 [J]. 控制理论与应用, 2007, 24(6): 873 – 878.)

[13] FIERRO R, LEWIS F L. Control of a nonholonomic mobile robot: backstepping kinematics into dynamics [J]. *Journal of Robotics Systems*, 1997, 14(3): 149 – 163.

[14] SOUSA C D, HEMERLY E M, GALVAO R K H. Adaptive control for mobile robot using wavelet networks [J]. *IEEE Transactions on System, Man and Cybernetics*, 2002, 32(4): 493 – 504.

[15] YOO S J, CHOI Y H, PARK J B. Generalized predictive control based on self-recurrent wavelet neural network for stable path tracking of mobile robots: adaptive learning rates approach [J]. *IEEE Transactions on Circuits and Systems*, 2006, 53(6): 1381 – 1394.

[16] DAS T, I KAR N, CHAUDHURY S. Simple neuron-based adaptive controller for a nonholonomic mobile robot including actuator dynamics [J]. *Neurocomputing*, 2006, 69(16/17/18): 2140 – 2151.

[17] DO K D, JIANG Z P, PAN J. Simultaneous tracking and stabilization of mobile robots: an adaptive approach [J]. *IEEE Transactions on Automatic Control*, 2004, 49(7): 1147 – 1152.

[18] DIXON W E, QUEIROZ M S, DAWSON D M, et al. Adaptive tracking and regulation of a wheeled mobile with controller/update law modularity [J]. *IEEE Transactions on Control Systems Technology*, 2004, 12(1): 138 – 147.

[19] DONG W, KUHNERT K D. Robust adaptive control of nonholonomic mobile robot with parameter and nonparameter uncertainties [J]. *IEEE Transactions on Robotics*, 2005, 21(2): 261 – 266.

[20] YANG J M, KIM J H. Sliding mode control of trajectory tracking of nonholonomic wheeled mobile robots [J]. *IEEE Transactions on Robotics and Automation*, 1999, 15(3): 578 – 587.

[21] CHWA D. Sliding-mode control of nonholonomic wheeled mobile robots in polar coordinates [J]. *IEEE Transactions on Control Systems Technology*, 2004, 12(4): 637 – 644.

[22] PARK B S, S YOO J, PARK J B, et al. Adaptive neural sliding-mode control of nonholonomic wheeled mobiles robots with model uncertainty [J]. *IEEE Transactions on Control Systems Technology*, 2009, 17(1): 207 – 214.

[23] CHEN C Y, LI T H S, YEH Y C, et al. Design and implementation of an adaptive sliding-mode dynamic controller for wheeled mobile robots [J]. *Mechatronics*, 2009, 19(2): 156 – 166.

[24] ZHENG Zewei, HUO Wei, ZHU Bing. Global path-following control for nonholonomic mobile robot [J]. *Control Theory & Applications*, 2012, 29(6): 741 – 746.
(郑泽伟, 霍伟, 诸兵. 非完整移动机器人全局路径跟踪控制 [J]. 控制理论与应用, 2012, 29(6): 741 – 746.)

[25] ANTONELLI G, CHIAVERINI S, FUSCO G. Real-time path tracking for unicycle-like mobile robots under velocity and acceleration constraints [C] //*Proceedings of the American Control Conference*. Arlington: ACC, 2001, 6: 119 – 124.

[26] ANTONELLI G, CHIAVERINI S, FUSCO G. A fuzzy-logic-based approach for mobile robot path tracking [J]. *IEEE Transactions on Fuzzy Systems*, 2007, 15(2): 211 – 221.

[27] MAALOUF E, SAAD M, SALIAH H. A higher level path tracking controller for a four-wheel differentially steered mobile robot [J]. *Robotics and Autonomous Systems*, 2006, 54(1): 23 – 33.

[28] MOUSTRIS G P, TZAFESTAS S G. Switching fuzzy tracking control for mobile robots under curvature constraints [J]. *Control Engineering Practice*, 2011, 9(1): 45 – 53.

[29] SU Y X, DUAN B Y, ZHENG C H, et al. Disturbance rejection high precision motion control of a Stewart platform [J]. *IEEE Transactions on Control Systems Technology*, 2004, 12(3): 364 – 374.

[30] SU Y X, ZHENG C H, DUAN B Y. Automatic disturbances rejection controller for precise motion control of permanent – magnet synchronous motors [J]. *IEEE Transactions on Industrial Electronics*, 2005, 52(3): 814 – 823.

[31] HAN J Q, YUAN L L. The discrete form of tracking-differentiator [J]. *Journal of Mathematics and System Science*, 1999, 19(3): 268 – 273.

[32] JANABI-SHARIFI F, HAYWARD V, CHEN C S J. Discrete-time adaptive windowing for velocity estimation [J]. *IEEE Transactions on Control Systems Technology*, 2000, 8(6): 1003 – 1009.

[33] JARITZ A, SPONG M W. An experimental comparison of robust control algorithms on a direct drive manipulator [J]. *IEEE Transactions on Control Systems Technology*, 1996, 4(6): 627 – 640.

[34] YAN C X, ZHAN Q. Real-time multiple mobile robots visual detection system [J]. *Sensor Review*, 2011, 31(3): 228 – 238.

作者简介:

张　弛 (1976–), 男, 博士研究生, 主要研究方向为微机电系统, E-mail: chizhang2008@163.com.